

Submitted to Journal of Bioinformatics and Computational Biology

**REGULARIZATION STRATEGIES FOR HYPERPLANE
CLASSIFIERS: APPLICATION TO CANCER CLASSIFICATION
WITH GENE EXPRESSION DATA**

ERIK ANDRIES

*Departments of Mathematics & Statistics and Pathology
University of New Mexico, Albuquerque, NM 87131, USA
andriese@math.unm.edu*

THOMAS HAGSTROM

*Department of Mathematics & Statistics
University of New Mexico, Albuquerque, NM 87131, USA
hagstrom@math.unm.edu*

SUSAN R. ATLAS

*Center for Advanced Studies and Department of Physics & Astronomy
University of New Mexico, Albuquerque, NM 87131, USA
susie@sapphire.phys.unm.edu*

CHERYL WILLMAN

*Cancer Research and Treatment Center and Department of Pathology
University of New Mexico, Albuquerque, NM 87131, USA
cwillman@salud.unm.edu*

Received (Day Month Year)

Revised (Day Month Year)

Accepted (Day Month Year)

Linear discrimination, from the point of view of numerical linear algebra, can be treated as solving an ill-posed system of linear equations. In order to generate a solution that is robust in the presence of noise, these problems require regularization. Here, we examine the ill-posedness involved in the linear discrimination of cancer gene expression data with respect to outcome and tumor subclasses. We show that a filter factor representation, based upon Singular Value Decomposition, yields insight into the numerical ill-posedness of the hyperplane-based separation when applied to gene expression data. We also show that this representation yields useful diagnostic tools for guiding the selection of classifier parameters, thus leading to improved performance.

Keywords: Singular value decomposition; least squares; regression; cancer classification; gene expression; regularization

1. Introduction

A current challenge in cancer treatment is to target specific therapies to distinct tumor types and to tailor the intensity of the treatment to the risk of relapse for each patient^{8,32,33}. Crucial to this effort is to effectively classify patients into specific risk groups. Traditionally, many risk stratification schemes use tumor morphology, molecular genetics and cytogenetics in addition to utilizing information such as race, age, etc.³⁵ Clinically, however, this approach has limitations. Tumors with similar appearances may have different clinical courses and display different responses to therapy. In addition, conventional laboratory diagnostic procedures do not reveal the full underlying molecular heterogeneity of these tumors. For this reason, there has been great interest in using gene arrays to identify more precisely known tumor subclasses, to discover new tumor subclasses, and to predict *outcome*, *i.e.* whether or not a patient's cancer will go into remission.

Our goal in this work is to investigate the classification of cancer patient samples according to tumor lineage and outcome via hyperplane classifiers, *i.e.* we attempt to linearly separate with a hyperplane patient samples via their expression profiles. This is numerically challenging since gene expression data is characterized by a noisy, high-dimensional, low-sample-size setting. Hyperplane classifiers cope with this challenging setting by incorporating prior knowledge assumptions that constrain the solution (the hyperplane parameters) in some way. The term *regularization* refers to this incorporation of prior information in order to stabilize the problem and to sift out a desired solution. With respect to hyperplane classifiers, there are many choices but each one encodes a different strategy for how to stabilize the solution, and, in this paper, we focus on the *filter factor representation* using singular value decomposition (SVD) as the particular regularization strategy. While some researchers have used SVD-based approaches^{14,27} for cancer classification, to the best of our knowledge, there has been no work on differentiating these methods on the basis of a filter factor representation. In addition, in seeking to evaluate why a certain regularization strategy should be preferred over another in the context of gene expression data, the type of numerical ill-posedness (*rank-deficiency* or *discrete ill-posedness*) exhibited by expression data ought to be taken into account. To date, this has not been done. Moreover, the filter factor representation involves the use of *spectral coefficients* that can be used to estimate how much regularization should be applied.

In Section 2, the mathematical notation used in subsequent sections will be detailed. In Section 3, we discuss kernel versions of regression-based hyperplane classifiers and the regularization approaches that these hyperplane classifiers can adopt when using a SVD-based filter factor representation. In Section 4, we review the cancer expression data sets used in our analysis and the methods used for data preprocessing and parameter estimation. Section 5 presents the classification results for hyperplane classifiers across a variety of regularization schemes and describes how spectral coefficients such as the singular values and Fourier coefficients can be

used to tune classifier parameters. Finally, we present the conclusion in 6.

2. Notation

The matrix $\mathbf{X} = [\mathbf{x}_1, \dots, \mathbf{x}_n] \in \mathbb{R}^{d \times n}$ denotes the gene expression data derived from n patient tissue samples with each patient expression vector $\mathbf{x}_i \in \mathbb{R}^d$ consisting of d gene attributes. The vector $\mathbf{y} \in \mathbb{R}^n$ consists of n binary-valued class labels where $y_i = \{-1, +1\}$ indicates membership in either the negative or positive class. With respect to acute leukemias, for example, one might assign the class label $y_i = -1$ or $y_i = +1$ to indicate membership in either ALL (acute lymphoblastic leukemia) or AML (acute myeloid leukemia), respectively. The matrix \mathbf{Y} is an $n \times n$ diagonal matrix such that $\mathbf{Y} = \text{diag}(\mathbf{y}) = \text{diag}(y_1, \dots, y_n)$ and $\mathbf{Y}^2 = \mathbf{I}_n$. The vectors $\mathbf{1}_n$ and $\mathbf{0}_n$ represent column vectors of n ones and zeros, respectively. The transpose of a matrix or vector is denoted by the superscript T , while $\|\cdot\|_2$ denotes the two-norm of a vector. The superscript p will refer to a specific partition of patient samples into a training and test set (this will be explained further in §5).

Given \mathbf{X} and \mathbf{y} , one attempts to learn the coefficients, $\mathbf{w} \in \mathbb{R}^d$ and w_0 , that determine a separating hyperplane given by the following mathematical expression: $g(\mathbf{x}) = \mathbf{x}^T \mathbf{w} + w_0 = 0$ ⁹. Geometrically, different choices of \mathbf{w} and w_0 typically yield different hyperplanes since \mathbf{w} determines the tilt of the hyperplane, while w_0 is the bias, or offset from the origin. To simplify notation, the data is often augmented to incorporate w_0 : $\hat{\mathbf{w}} = [\mathbf{w}^T, w_0]^T \in \mathbb{R}^{d+1}$ and $\hat{\mathbf{x}} = [\mathbf{x}^T, 1]^T \in \mathbb{R}^{d+1}$ denote augmented weight and gene expression vectors, respectively. Hence, $g(\mathbf{x}) = \mathbf{x}^T \mathbf{w} + w_0$ can be simply expressed as $g(\mathbf{x}) = \hat{\mathbf{x}}^T \hat{\mathbf{w}}$. Similarly, $\hat{\mathbf{X}} = [\mathbf{X}^T, \mathbf{1}_n]^T \in \mathbb{R}^{(d+1) \times n}$ is the augmented data for the entire gene expression matrix. This augmentation adds a constant feature to the training data such that the separating hyperplane passes through the origin in \mathbb{R}^{d+1} . The algorithm that determines the optimal hyperplane parameters $\hat{\mathbf{w}}$ will be referred to as a *hyperplane classifier*, and the data \mathbf{X} and \mathbf{y} used to determine $\hat{\mathbf{w}}$ is referred to as the *training data*. Once $\hat{\mathbf{w}}$ is obtained, the formal classification task is to assign class membership to a new input $\mathbf{z} \in \mathbb{R}^d$: if $g(\mathbf{z}) < 0$ ($g(\mathbf{z}) > 0$), then \mathbf{z} is assigned to the negative (positive) class. If $g(\mathbf{z}) = 0$, then the class membership of \mathbf{z} is indeterminate. If $\hat{\mathbf{Z}} = [\hat{\mathbf{z}}_1, \dots, \hat{\mathbf{z}}_N] \in \mathbb{R}^{(d+1) \times N}$ consists of N augmented test set expression profiles distinct from the training set and $\mathbf{t} \in \mathbb{R}^N$ is its corresponding set of class labels such that $t_i = \{-1, +1\}$, then the number of misclassifications M can be computed as follows:

$$M = \sum_{i=1}^N I[t_i g(\hat{\mathbf{z}}_i)] = \sum_{i=1}^N I[t_i (\hat{\mathbf{z}}_i^T \hat{\mathbf{w}})] \quad (1)$$

where $I[\cdot]$ is the indicator function such that $I[\theta] = 1$ if $\theta < 0$ and $I[\theta] = 0$ if $\theta \geq 0$.

3. Filter Factor Representations of Hyperplane Classifiers

A hyperplane classifier, in its simplest form, specifies a linear relationship between a response variable, \mathbf{y} , and a set of predictor variables, \mathbf{X} . For many problems,

estimates of the linear relationships between variables are adequate to describe the observed data and to make reasonable predictions for new observations. This has been well-established in the case of cancer classification using gene expression data.^{14,23,24,27} However, since the number of samples (n) is much less than the number of genes (d), the samples sparsely populate a very high dimensional gene space and, as a result, there is a strong likelihood of finding many perfectly separating hyperplanes for the training data. Another complicating factor is the presence of significant biological and experimental variability in the expression data. Assuming that a linear discrimination approach to the classification of gene expression data will generally suffice, we therefore focus on deciding which regularization strategy is appropriate for extracting a *stable* set of hyperplane parameters in the presence of noisy and high-dimensional data.

3.1. Kernel-based regression

Suppose that the hyperplane classifier attempts to find $\hat{\mathbf{w}}$ by solving the regression problem $\hat{\mathbf{X}}^T \hat{\mathbf{w}} = \mathbf{y}$ using least squares (LS) minimization:

$$\min_{\hat{\mathbf{w}}} \left\| \hat{\mathbf{X}}^T \hat{\mathbf{w}} - \mathbf{y} \right\|_2^2 = \min_{\hat{\mathbf{w}}} \sum_{i=1}^n (\hat{\mathbf{x}}_i^T \hat{\mathbf{w}} - y_i)^2 = \min_{\hat{\mathbf{w}}} \sum_{i=1}^n (g(\hat{\mathbf{x}}_i) - y_i)^2 \quad (2)$$

LS methods for solving for the weight vector $\hat{\mathbf{w}}$ (hereafter referred to as the *primal variable*), such as QR factorization, involve $O(dn^2)$ floating point operations (*flops*)¹⁰. When $d \gg n$, one can reduce the computational complexity by working with the kernel version of Eq.(2) instead. Assuming that $\hat{\mathbf{w}}$ can be rewritten as a linear combination of the training data, *i.e.*, $\hat{\mathbf{w}} = \hat{\mathbf{X}}\boldsymbol{\beta}$, $\boldsymbol{\beta} \in \mathbb{R}^n$, $\boldsymbol{\beta}$ (hereafter referred to as the *dual variable*) can be determined instead:

$$\min_{\hat{\mathbf{w}}} \left\| \hat{\mathbf{X}}^T \hat{\mathbf{w}} - \mathbf{y} \right\|_2^2 = \min_{\boldsymbol{\beta}} \left\| \hat{\mathbf{X}}^T (\hat{\mathbf{X}}\boldsymbol{\beta}) - \mathbf{y} \right\|_2^2 = \min_{\boldsymbol{\beta}} \|\mathbf{K}\boldsymbol{\beta} - \mathbf{y}\|_2^2, \quad (3)$$

where $\mathbf{K} = \hat{\mathbf{X}}^T \hat{\mathbf{X}} \in \mathbb{R}^{n \times n}$ will be referred to as the linear *kernel* matrix. Solving Eq.(3) now scales cubically with the number of patient samples n .

3.2. Need for regularization

If $\hat{\mathbf{X}}$ is ill-conditioned, then the computed solution $\boldsymbol{\beta}$ will not be stable. Ill-conditioning is always the case with coefficient matrices derived from classification-based regression problems. For example, if $\hat{\mathbf{X}} = [\hat{\mathbf{X}}_+, \hat{\mathbf{X}}_-]$ is a data partitioning with respect to the positive and negative classes, then the feature or attribute profiles of data points within $\hat{\mathbf{X}}_+$ and $\hat{\mathbf{X}}_-$ will be highly correlated because it is this commonality which defines the class. As a result, the effective numerical rank r_{eff} (the number of columns of $\hat{\mathbf{X}}$ that are linearly independent with respect to some error level) will be small due to the multicollinearity of the columns within $\hat{\mathbf{X}}_+$ and $\hat{\mathbf{X}}_-$. In the case of gene expression data, r_{obs} can vary significantly due to the

large amount of within-class and between-class biological variability. In addition, the large amount of noise associated with gene arrays can artificially inflate r_{eff} such that the observed rank r_{obs} will be greater than r_{eff} . In general, $r_{\text{obs}} = n$ (full rank) but $r_{\text{eff}} \ll r_{\text{obs}}$.

The phenomenon of solution instability can be illustrated by expressing the ordinary least squares (OLS) solution to Eq.(3) in terms of the singular value decomposition (SVD) of $\hat{\mathbf{X}}^{10,28}$. If $\hat{\mathbf{X}} = \mathbf{U}\mathbf{\Sigma}\mathbf{V}^T$ is the SVD of $\hat{\mathbf{X}}$, where

$$\begin{aligned} \mathbf{U} &= [\mathbf{u}_1, \dots, \mathbf{u}_n] \in \mathbb{R}^{(d+1) \times n}, \quad \mathbf{V} = [\mathbf{v}_1, \dots, \mathbf{v}_n] \in \mathbb{R}^{n \times n}, \\ \mathbf{U}^T \mathbf{U} &= \mathbf{V}^T \mathbf{V} = \mathbf{I}_n, \\ \mathbf{\Sigma} &= \text{diag}(\sigma_1, \dots, \sigma_n), \quad \sigma_1 \geq \dots \geq \sigma_n \geq 0, \end{aligned}$$

then the solution $\boldsymbol{\beta}$ can be given in terms of $\mathbf{\Sigma}$ and \mathbf{V} :

$$\boldsymbol{\beta} = \mathbf{K}^{-1} \mathbf{y} = \mathbf{V} \mathbf{\Sigma}^{-2} \mathbf{V}^T \mathbf{y} = \sum_{i=1}^n \left(\frac{\mathbf{v}_i^T \mathbf{y}}{\sigma_i^2} \right) \mathbf{v}_i. \quad (4)$$

Since we assumed $\hat{\mathbf{X}}$ to have full rank (even though it is ill-conditioned), we use \mathbf{K}^{-1} instead of replacing it with the pseudoinverse \mathbf{K}^\dagger . In Eq.(4), the terms associated with small singular values (*i.e.*, terms associated with large i) correspond to spurious noise inherent in the data. Division by small singular values unduly amplifies the effect of these noise terms and has a direct analogue with overfitting: if we include terms associated with small singular values, then the solution will have low *bias* and high *variance*²¹. Numerically, this overfitting will manifest itself as a large solution norm for $\boldsymbol{\beta}$ since $\|\boldsymbol{\beta}\|_2^2 = \sum_{i=1}^n [(\mathbf{v}_i^T \mathbf{y})/\sigma_i^2]^2$. Regularization in the context of the SVD expansion of Eq.(4) amounts to eliminating or damping noise terms associated with small singular values. This, in effect, imposes a prior knowledge assumption of ‘‘smoothness’’ on the solution since large values of $\|\boldsymbol{\beta}\|_2^2$ are penalized.

3.3. Filter factor representations

There are a variety of regularization techniques that can be used to impose solution smoothness. We are particularly interested in techniques that admit *filter factor solutions*¹⁹. A filter factor representation is a reweighting of Eq.(4) and has the form

$$\boldsymbol{\beta} = \mathbf{V} \mathbf{F} \mathbf{\Sigma}^{-2} \mathbf{V}^T \mathbf{y} = \sum_{i=1}^n \left(\frac{\mathbf{v}_i^T \mathbf{y}}{\sigma_i^2} \right) f_i \mathbf{v}_i, \quad (5)$$

where $\mathbf{F} = \text{diag}(f_1, \dots, f_n)$ is a diagonal matrix consisting of the *filter factors*¹⁹ or *shrinkage coefficients*²¹. The filter factors typically decay to zero as i increases such that contributions from terms with small singular values are filtered out. For the OLS solution, no damping occurs since $\mathbf{F} = \mathbf{I}_n$ (or $f_1 = \dots = f_n = 1$). However, least squares (LS) techniques such as truncated singular value decomposition (TSVD), kernel ridge regression (KRR) and partial least squares (PLS) have non-trivial filter factor representations as a result of solving a modified LS problem

involving the dual variable β . Each of these LS methods, through its respective filter factor representation, encodes a different regularization strategy in order to suppress the noisy terms in the SVD expansion of Eq.(4). We briefly describe each of these methods in turn.

3.3.1. TSVD

For TSVD, the approach to damping noise terms in Eq.(4) is to simply eliminate them entirely. Keeping the first k terms amounts to having binary-valued filter factors such that $f_1 = \dots = f_k = 1$ and $f_{k+1} = \dots = f_n = 0$. Alternatively, one can arrive at the same solution by solving the modified LS problem, $\mathbf{K}_k \beta = \mathbf{y}$, in which $\mathbf{K}_k = \sum_{i=1}^k \sigma_i \mathbf{v}_i \mathbf{v}_i^T$ is the rank- k approximation of \mathbf{K} obtained by replacing the smallest $n - k$ singular values with zeros.

3.3.2. KRR

For KRR, the modified LS problem involving β is derived by minimizing the following loss function, $L(\hat{\mathbf{w}}) = \|\hat{\mathbf{X}}^T \hat{\mathbf{w}} - \mathbf{y}\|_2^2 + \lambda^2 \|\hat{\mathbf{w}}\|_2^2$, by setting $\nabla_{\hat{\mathbf{w}}} L(\hat{\mathbf{w}}) = \mathbf{0}_{d+1}$ and replacing $\hat{\mathbf{w}}$ with $\hat{\mathbf{X}} \beta$:

$$\nabla_{\hat{\mathbf{w}}} L(\hat{\mathbf{w}}) = 2(\hat{\mathbf{X}} \hat{\mathbf{X}}^T + \lambda^2 \mathbf{I}_{d+1}) \hat{\mathbf{w}} - 2\hat{\mathbf{X}} \mathbf{y} = \mathbf{0}_{d+1} \Rightarrow (\mathbf{K} + \lambda^2 \mathbf{I}_n) \beta = \mathbf{y}. \quad (6)$$

Note, however, that the linear system in Eq.(6) involving β is not of the form typically associated with classical ridge regression or Tikhonov regularization,

$$(\mathbf{A}^T \mathbf{A} + \gamma^2 \mathbf{B}^T \mathbf{B}) \mathbf{x} = \mathbf{A}^T \mathbf{b}, \quad (7)$$

in which the matrices $\mathbf{A} \in \mathbb{R}^{m \times n}$ and $\mathbf{B} \in \mathbb{R}^{n \times p}$ ($m \geq n \geq p$) are not assumed to be symmetric positive definite (SPD). Instead, $(\mathbf{K} + \lambda^2 \mathbf{I}_n) \beta = \mathbf{y}$ corresponds to a related regularization scheme first proposed by Franklin¹² (hereafter referred to as the *Franklin* regularization scheme) in which he suggested replacing Eq.(7) with

$$(\mathbf{A} + \gamma \mathbf{B}) \mathbf{x} = \mathbf{b}, \quad \gamma > 0, \quad (8)$$

when $\mathbf{A} \in \mathbb{R}^{n \times n}$ and $\mathbf{B} \in \mathbb{R}^{n \times n}$ are SPD. If $\mathbf{B} = \mathbf{I}_n$ and $\{\psi_1, \dots, \psi_n\}$ are the singular values of \mathbf{A} , then the filter factors are the following¹⁹:

$$f_i = \begin{cases} \psi_i^2 / (\psi_i^2 + \gamma^2), & \text{Tikhonov regularization,} \\ \psi_i / (\psi_i + \gamma), & \text{Franklin regularization.} \end{cases}$$

Hence, KRR, in the context of Eq.(7), is nothing more than the Franklin regularization scheme with $\mathbf{A} \equiv \mathbf{K}$ (where $\psi_i = \sigma_i^2$), $\mathbf{B} \equiv \mathbf{I}_n$, $\mathbf{x} \equiv \beta$, $\mathbf{b} \equiv \mathbf{y}$ and $\gamma \equiv \lambda^2$.

In the context of support vector machine (SVM) classification⁹, KRR also has connections with the *two-norm* SVM formulations, namely, Proximal SVM (PSVM)¹³ and Lagrangian SVM (LSVM)²⁶. Cast as an optimization problem, the

objective functions associated with these particular SVM formulations are identical, while the constraints differ slightly:

$$\min_{\hat{\mathbf{w}}} \frac{1}{2} \|\hat{\mathbf{w}}\|_2^2 + \frac{\nu}{2} \|\boldsymbol{\xi}\|_2^2 \quad \text{s.t.} \quad \begin{cases} \mathbf{Y} \left(\hat{\mathbf{X}}^T \hat{\mathbf{w}} \right) + \boldsymbol{\xi} \geq \mathbf{1}_n \text{ (LSVM)} \\ \mathbf{Y} \left(\hat{\mathbf{X}}^T \hat{\mathbf{w}} \right) + \boldsymbol{\xi} = \mathbf{1}_n \text{ (PSVM)} \end{cases} \quad (9)$$

where $\boldsymbol{\xi} \in \mathbb{R}^n$ is a vector of slack variables⁷ and ν is a parameter which controls the overall amount of misclassification violation⁹. If the data points were linearly separable, the LSVM would require that all of the data points lie outside of the corridor defined by $g(\mathbf{w}) = \hat{\mathbf{x}}^T \hat{\mathbf{w}} < 1$. Numerically, this is described by the set of constraints:

$$\mathbf{Y} \left(\hat{\mathbf{X}}^T \hat{\mathbf{w}} \right) \geq \mathbf{1}_n. \quad (10)$$

However, for data sets that are not linearly separable, the constraints in Eq.(10) are never simultaneously satisfied. To allow for the likely possibility of data points lying on the wrong side of the separating hyperplane (or allowing for *slackness* in the constraints), $\boldsymbol{\xi}$ and ν are introduced to allow for the violation of Eq.(10). In effect, one can view the LSVM relaxation of the inequality constraints as a regularization mechanism which imposes a “smoothness” prior on the solution $\hat{\mathbf{w}}$. The corresponding *dual* version of Eq.(9), obtained using the Karush-Kuhn-Tucker conditions of optimization theory⁷, can then be expressed, after some algebraic manipulation, as the following constrained LS problem,

$$\text{solve } (\mathbf{K} + \lambda^2 \mathbf{I}_n) \boldsymbol{\beta} = \mathbf{y} \quad \text{s.t.} \quad \begin{cases} \mathbf{Y} \boldsymbol{\beta} \geq \mathbf{0}_n \text{ (LSVM)} \\ \boldsymbol{\beta} \in \mathbb{R}^n \text{ (PSVM)}, \end{cases} \quad (11)$$

where $\lambda = 1/\nu$. For the PSVM, $\boldsymbol{\beta}$ is unconstrained in Eq.(11) and hence is equivalent to KRR (this was first observed by Agarwal²). For the LSVM, the data points associated with the nonzero component values of $\boldsymbol{\beta}$ are called the *support vectors*. Geometrically, these data points lie on or within the *canonical corridor* defined by $g(\mathbf{x}) = \hat{\mathbf{x}}^T \hat{\mathbf{w}} \leq 1$ and these points alone determine the orientation of the hyperplane since $\hat{\mathbf{w}} = \hat{\mathbf{X}} \boldsymbol{\beta} = \sum_{\beta_i \neq 0} \beta_i \hat{\mathbf{x}}_i$.

3.3.3. PLS

The Krylov subspace, $\mathcal{K}_m(\mathbf{A}, \mathbf{b}) = \text{span}\{\mathbf{b}, \mathbf{A}\mathbf{b}, \dots, \mathbf{A}^{m-1}\mathbf{b}\}$, is often associated with the conjugate gradient (CG) algorithm applied to $\mathbf{A}\mathbf{x} = \mathbf{b}$ when \mathbf{A} is SPD²⁸. In solving the regression problem $\hat{\mathbf{X}}^T \hat{\mathbf{w}} = \mathbf{y}$, Helland showed that the PLS-based weight vector $\hat{\mathbf{w}}$ lies in the Krylov subspace $\mathcal{K}_m(\hat{\mathbf{X}} \hat{\mathbf{X}}^T, \hat{\mathbf{X}} \mathbf{y})$ ²². If we express this Krylov subspace in terms of \mathbf{K} and $\boldsymbol{\beta}$, we have

$$\mathcal{K}_m(\hat{\mathbf{X}} \hat{\mathbf{X}}^T, \hat{\mathbf{X}} \mathbf{y}) = \text{span}\{\hat{\mathbf{X}} \mathbf{y}, \hat{\mathbf{X}} \mathbf{K} \mathbf{y}, \dots, \hat{\mathbf{X}} \mathbf{K}^{m-1} \mathbf{y}\} = \text{span}\{\hat{\mathbf{X}} \boldsymbol{\beta}\}, \quad (12)$$

where $\boldsymbol{\beta} \in \mathcal{K}_m(\mathbf{K}, \mathbf{y})$. As a result, the modified LS problem associated with PLS is

$$\mathbf{K} \boldsymbol{\beta} = \mathbf{y}, \quad \boldsymbol{\beta} \in \mathcal{K}_m(\mathbf{K}, \mathbf{y}).$$

The filter factors can then be expressed in terms of the Ritz polynomial, $p_m(\theta)^{25}$,

$$f_i = 1 - p_m(\sigma_i^2), \quad p_m(\theta) = \prod_{i=1}^n \left(\frac{\theta_i(m) - \theta}{\theta_i(m)} \right), \quad (13)$$

a consequence of the Lanczos tridiagonalization process inherent in the CG algorithm¹⁹. At step m , the Lanczos tridiagonalization produces a tridiagonal matrix \mathbf{T}_m by taking the QR factors of successive Krylov subspaces, $\mathbf{Q}_m \mathbf{R}_m := \mathcal{K}_m(\mathbf{K}, \mathbf{y})$, such that $\mathbf{T}_m = \mathbf{Q}_m^T \mathbf{K} \mathbf{Q}_m$ ²⁸. The eigenvalues of \mathbf{T}_m , denoted by $\theta_i(m)$, are called the Ritz values. The filtering properties of f_i are controlled by the convergence of θ_i^m to the nonzero eigenvalues of \mathbf{K} , *i.e.* $\text{diag}(\Sigma^2) = \{\sigma_1^2, \dots, \sigma_n^2\}$. This convergence, in turn, is controlled by the number of columns m spanned by the Krylov subspace. If $\theta_i(m)$ has converged to σ_i^2 , then $p_m(\theta_i(m)) = 0$ and $f_i = 1$. As m approaches n and if *all* of the Ritz values converge to their corresponding eigenvalues of \mathbf{K} , then all of the filter factors will approach one, and the PLS solution will coincide with the OLS solution. However, in practice, as m increases, one often gets multiple copies for large values of $\theta_i(m)$ (*ghost values*) due to finite-precision arithmetic²⁸. Hence, the Ritz values disproportionately converge to the largest eigenvalues of \mathbf{K} as m increases. This results in a delayed or lack of convergence of $\theta_i(m)$ toward σ_i^2 . Therefore, the PLS solution generally does not coincide in real computations with the OLS solution for $m = n$ since convergence to the smallest eigenvalues of \mathbf{K} is rarely achieved. As a result of the delayed convergence, an optimal or near optimal m often satisfies $m \ll n$ for ill-conditioned coefficient matrices \mathbf{K} —see Fig.(1).

3.3.4. *Nonstandard filter factor representations*

Filter factor representations can easily accommodate non-standard filtering procedures. Standard filtering procedures typically assume that, in the SVD expansion, the terms corresponding to the largest singular values are the most important and should be kept, while the terms corresponding to the smallest singular values should be filtered out or damped. This not need be the case with gene expression data. In Alter *et al.*³, the largest singular value and its corresponding right and left singular vectors were removed in order to filter out the steady state of yeast cell cycle expression. Bair *et al.*⁶ introduced a mixture model for outcome to accommodate other sources of non-outcome variation in which the outcome class label vector \mathbf{y} was expressed as a linear combination of the first two singular vectors: $\mathbf{y} \approx \alpha \mathbf{u}_1 + (1 - \alpha) \mathbf{u}_2 + \boldsymbol{\epsilon}_n$, $\alpha \in [0, 1]$, where $\boldsymbol{\epsilon}_n$ is an $n \times 1$ error vector in which each component value is Gaussian with unit variance. When $\alpha = 1$ and $\alpha = 0$, \mathbf{y} is correlated with \mathbf{u}_1 and \mathbf{u}_2 , respectively, since $\boldsymbol{\beta} = \mathbf{U} \mathbf{F} \Sigma^{-2} \mathbf{U}^T \mathbf{y} \approx [f_1/\sigma_1^2] \alpha \mathbf{u}_1 + [f_2/\sigma_1^2] (1 - \alpha) \mathbf{u}_2$. Hence, for $\alpha = 1$, we have $f_1 \approx 1$ and $f_{i \neq 1} \approx 0$, while for $\alpha = 0$, we have, $f_2 \approx 1$ and $f_{i \neq 2} \approx 0$.

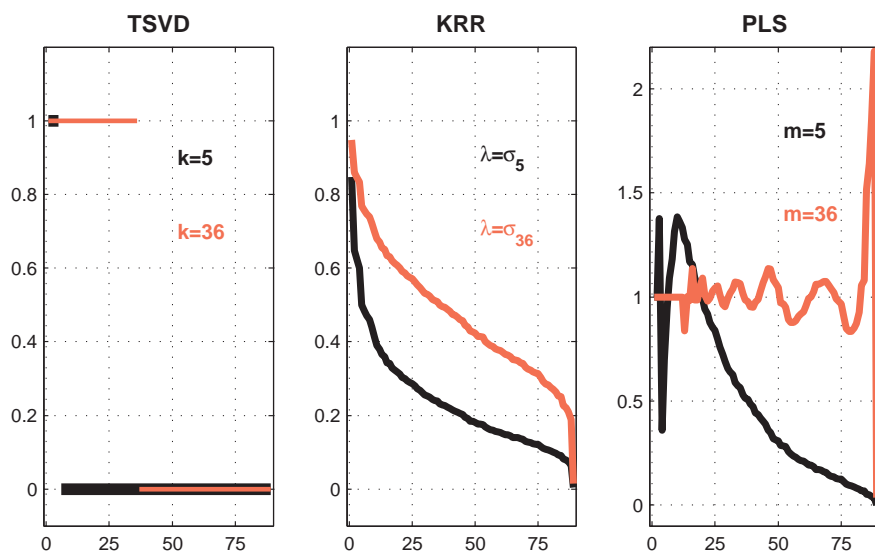
3.4. Extent of regularization

For TSVD, KRR and PLS, one must decide upon the value of k (the number of singular values and vectors kept in the SVD expansion of Eq.(4)), λ (the multiplicative factor of the identity matrix added to \mathbf{K} in Eq.(6)) and m (the number of columns spanned by the Krylov subspace \mathcal{K}_m) using information obtained from the training data only. The choice of the regularization parameter dictates the values of the filter factors which, in turn, control the amount of smoothing the solution β will undergo. For TSVD and PLS, the regularization parameters k and m are the integer-valued entities $\{1, 2, \dots, n\}$, and the smaller the regularization parameter, the greater the amount of smoothing. A regularization parameter of n effectively amounts to an absence of regularization since $f_i \approx O(1)$ for any $i \in \{1, 2, \dots, n\}$. For KRR, however, the regularization parameter λ is nonnegative and real-valued—the larger the value, the greater the amount of smoothing and vice-versa. In particular, the effective range of regularization for λ lies in the interval $[0, \sigma_1]$ since $\lambda = 0$ corresponds to no regularization ($f_1 = \dots = f_n = 1$) while $\lambda = \sigma_1$ roughly amounts to keeping the first term of the SVD expansion ($f_1 = 1/2 \approx O(1)$ and $f_i \approx O(\epsilon)$ for $i \geq 2$ and $0 < \epsilon \ll 1$). Note that for TSVD and KRR, the filter factors lie within the interval $[0, 1]$; see Fig.(1). From the point of view of regularization, this makes perfect sense since we either want to keep an SVD expansion term ($f_i \approx 1$) or suppress an SVD expansion term ($f_i \approx 0$). However, the filter factors for PLS can lie outside of $[0, 1]$ since $f_i = 1 - p_m(\sigma_i^2)$ is a polynomial of degree m and can assume large positive and negative values as $p_m(\theta)$ oscillates; see Fig.(1). Hence, the regularization effects of PLS can be difficult to interpret. Additional details of the regularizing effects of the CG algorithm in the context of PLS can be found in the work of Lingjærde and Christopherson²⁵.

3.5. Choice of filter factors and ill-posedness

The choice of filter factors should be informed by the type of numerical ill-posedness exhibited by $\hat{\mathbf{X}}$. There are generally two types of numerical ill-posedness in the case of linear systems: *rank-deficiency* and *discrete ill-posedness*¹⁹. Rank-deficiency is characterized by a large gap between σ_k and σ_{k+1} in the singular value spectrum of $\hat{\mathbf{X}}$ in which the last $n - k$ singular values are assumed to reflect spurious noise inherent in the data. In this case, $r_{\text{eff}} = k$ and the preferred treatment for handling such ill-posedness is the TSVD scheme: truncate the last $n - k$ terms in the SVD expansion. On the other hand, discrete ill-posedness is characterized by a slow decay of the singular values in which there is no well-determined gap in the singular value spectrum. For such problems, truncation of the SVD expansion may not lead to the best-regularized solution. If we truncate too early, then we may lose information, and if we include too many terms, then the solution can become unstable in the presence of noise. As a result, one may want to compromise by reweighting all of the terms such that terms with small singular values are damped to a greater degree than terms with larger singular values. In this case, the preferred remedy would

Fig. 1. Comparison of various filter factors representations for the training data in the normalized **UNM Infant ALL/AML** data set (see §4). The filter factors f_i (y -axes) are plotted against the summation index i (x -axes). The regularization parameters for TSVD, KRR and PLS are $k = \{5, 36\}$ (the truncation parameters), $\lambda \in \{\sigma_5, \sigma_{36}\}$ (the scalar multiples of the identity matrix, \mathbf{I}_n) and $m \in \{5, 36\}$ (the number of columns spanning the Krylov subspace, $\mathcal{K}_m(\mathbf{K}, \mathbf{y})$).



be either KRR or PLS. In this study, we are interested in whether the type of numerical ill-posedness exhibited by the cancer gene expression data should dictate the type of regularization scheme used and whether this leads to improvement in overall classification performance. We now discuss our numerical results for several cancer gene expression data sets.

4. Gene Expression Data Sets and Preprocessing

4.1. Gene expression data sets

Over the past several years, there have been a number of human gene expression studies that have considered the problem of classification with respect to tumor lineage and outcome. This paper focuses on the following data sets:

- **UNM Infant ALL/AML**³⁰: In this study, 126 infant (< 1 year) samples were grouped according to their major precursor origins within acute leukemia: acute lymphoblastic leukemia (ALL) and acute myeloid leukemia (AML).
- **MIT-ALL/AML**¹⁵: In this study, 72 patient samples were grouped according to ALL or AML.
- **UNM Pediatric ALL Outcome**²⁹: 254 pediatric patient samples (< 18 years of age) with ALL were examined with respect to outcome. This data set includes distinct tumor sublineages (34 T-cell ALL and 220 B-cell ALL patient samples) and multiple molecular subtypes (the chromosomal aberrations that give rise to certain leukemias).
- **van't Veer Breast Cancer Outcome**³²: This data set concerns primary breast cancer outcome (patients who remained metastasis-free for at least five years versus those patients who developed distant metastases within five years) in a group of 95 patients selected for age (< 55 years) and a clinical indication of favorable prognosis (*i.e.* lymph node negative status and a tumor diameter less than 5 centimeters).

The class distribution of the patient samples across the cancer gene expression data sets can be found in Table 1. The **UNM Infant ALL/AML** and the **UNM Pediatric ALL Outcome** data sets used the Affymetrix MAS 5.0 software¹ to generate expression levels for 12625 genes (actually cDNA probesets), while for the **MIT ALL/AML** data set, the Affymetrix MAS 4.0 software was used to generate expression values for 7129 genes. For the **van't Veer Breast Cancer Outcome** data set, spotted gene arrays (Hu25K microarrays) containing 24,481 genes were used.

Table 1. Class distribution of patient samples across data sets.

Data Set	Training Set	Test Set
UNM Infant ALL/AML	54 ALL; 35 AML	24 ALL; 13 AML
MIT ALL/AML	27 ALL; 11 AML	20 ALL; 14 AML
UNM Pediatric ALL Outcome	73 REM; 94 FAIL	39 REM; 48 FAIL
van't Veer Breast Cancer Outcome	44 REM; 34 FAIL	7 REM; 12 FAIL

These gene array data sets were chosen since we wanted to consider class prediction tasks based upon tumor lineage and outcome. In approximate terms, tumor lineage and outcome are opposites with respect to the observed biological variability. We expect tumor lineage to have a higher signal-to-noise ratio than outcome since tumor lineage dominates the fate of cancer cells. Conversely, outcome embodies the full biological, genomic and environmental heterogeneity of an individual, making it difficult to isolate a unique or universal favorable or unfavorable signature within

the biological noise. Since hyperplane classifiers differ in how they stabilize the solution in the presence of noise, certain hyperplane classifiers may be better-suited to handling class prediction tasks that differ in signal-to-noise ratios.

4.2. Gene selection

In cancer gene expression studies, not all genes change substantially in response to disease. As a result, a filtering procedure is often used to reduce the total of number of genes, d , to a core subset in which the reduced number of genes, denoted by d' , are differentially expressed with respect to the class distinction of interest. Here, a two-stage filtering procedure is used. First, genes are removed on the basis of qualitative measures of gene detection. Second, highly discriminating genes are chosen using a ranking procedure based upon weight-vector component magnitudes.

For the data sets using the Affymetrix platform, all control genes/probesets were removed, *i.e.* all probesets having the “AFFX” prefix in the probeset ID¹. In addition, any probeset that did not have at least one “Present” *call value* (as determined by the Affymetrix MAS 5.0 statistical software) within the training set samples was also removed. A call value is an Affymetrix-specific qualitative measure of detection: it indicates whether a gene was expressed (“present”), was not expressed (“absent”) or was too close to call (“marginal”). This typically reduces the initial number of probesets by a third or a quarter. For the **van’t Veer Breast Cancer Outcome** data set (the only non-Affymetrix-based data set), two patients (samples 53 and 54) had a significant number of missing values and these two samples were excluded from subsequent analysis (this was not done in the study of van’t Veer *et al.*³²). A gene was then removed if there was at least one missing expression value among all of the training set samples. Note: If one of the genes in the test set had a missing value, then the missing value for that gene was replaced with the mean of the normalized expression values for that gene in the training set; see §4.3 for data normalization details.

For the second stage of the gene selection process, a modified version of the Recursive Feature Elimination (RFE) algorithm¹⁸ was used. In the RFE algorithm, an SVM (or any other hyperplane classifier for that matter) is trained using all of the genes from patient samples in the training set. The genes are then ranked according to their largest weight-component magnitudes,

$$\{|w_{i_1}|, \dots, |w_{i_d}|\},$$

where $\{i_1, \dots, i_d\}$ are the sorting indices such that $|w_{i_1}|$ and $|w_{i_d}|$ are the largest and smallest weight-component magnitudes, respectively. The genes associated with the smallest weight-component magnitudes are removed and the SVM is then retrained using the remaining genes. This process is repeated iteratively until there are no more genes left. Here, we use KRR to generate the weight vector per iteration: $\hat{\mathbf{w}}^{(k)} = \hat{\mathbf{X}}\boldsymbol{\beta}^{(k)}$ where $\boldsymbol{\beta}^{(k)}$ is the solution to the linear system,

$$(\mathbf{K}^{(k)} + \lambda^{(k)}\mathbf{I}_n)\boldsymbol{\beta}^{(k)} = \mathbf{y},$$

k is the RFE iteration and $\mathbf{K}^{(k)}$ is the kernel matrix obtained using only the gene subset obtained at iteration k . In the previous work of Guyon *et al.*¹⁸, the regularization parameter λ was fixed across all gene subsets. This strategy tends to under-regularize (over-regularize) $\mathbf{K}^{(k)}$ when k is small (large). Here, we modify the regularization parameter $\lambda^{(k)}$ to be the mean of the singular values of $\mathbf{K}^{(k)}$ (or equivalently, the mean of the trace of $\mathbf{K}^{(k)}$). This allows for *fast* computation (no SVD of $\mathbf{K}^{(k)}$ is required) and *consistent* filtering across RFE iterations. This filtering also intentionally errs on the side of over-regularization since $\lambda^{(k)}$ is weighted toward the largest singular values (otherwise, if $\lambda^{(k)}$ is too small, then we will under-regularize $\mathbf{K}^{(k)}$ and overfit the training data).

In this study, the number of genes used in the hyperplane classifier is varied amongst the values in the set: $d' = \{d(\text{all genes}), 100, 50, 25, 10\}$. Our interest is not in finding the optimal subset of discriminating genes, but in measuring qualitative changes of class prediction performance as d' is decreased. Removing spurious “gene noise” is a common and valid reason given for using gene selection. However, there are other more practical reasons for doing so. Computationally, gene selection greatly eases the numerical burden in, say, computing the SVD of $\tilde{\mathbf{X}}$. Clinically, assays that require relatively few gene expression levels to be measured are more likely to be adopted in a real-world setting.

4.3. Data normalization

Expression values corresponding to different genes can differ significantly in magnitude. As a result, one often tries to transform and scale the data such that the expression values across patients for a given gene are of the same size. First, the expression data was *log*-transformed using the transformation, $\mathbf{x}_{ij} \leftarrow \text{sgn}(x_{ij}) \log_2(|x_{ij}|)$, since the data tends to exhibit a log-normal distribution for the *positive* values for a fixed gene (note that for the **van’t veer Breast Cancer Outcome** data set, the publically-available data was already log-transformed). Second, the expression values for a fixed gene across the training set samples were normalized to mean zero and unit standard deviation (the expression values for a fixed gene within the test set were normalized using the mean and standard deviation from the training set). Third, to avoid scaling problems when solving $\mathbf{K}\boldsymbol{\beta} = \mathbf{y}$, both \mathbf{K} and \mathbf{y} were re-scaled so that their component elements were of commensurate size. Following the recommendation of Varah³¹, the left- and right-hand sides of $\mathbf{K}\boldsymbol{\beta} = \mathbf{y}$ were re-scaled such that $\|\mathbf{K}\|_2 = \sigma_1^2 \approx O(1) \approx \|\mathbf{y}\|_2^2$. This was easily accomplished using the following re-scaling: $\boldsymbol{\Sigma} \leftarrow \boldsymbol{\Sigma}/\sigma_1$ and $\mathbf{y} \leftarrow \mathbf{y}/\sqrt{n}$.

4.4. Model Selection

N -fold cross-validation was used to estimate the value of the regularization parameter. In this study, we used $N = 10$. For TSVD and PLS, the candidate values used for k and m , respectively, came from the set $\{1, \dots, n\}$. The candidate values for

λ came from the set of singular values ($\lambda \in \{\sigma_1, \dots, \sigma_n\}$) since, for Tikhonov and Franklin regularization, the effective range for λ lies in the interval $[0, \sigma_1]$ ¹⁹. Due to the re-scaling of the data to obtain $\|\mathbf{K}\|_2^2 = \sigma_1^2 = 1$, the set of candidate values for λ lie in the interval $[0, 1]$. Note that in this study, gene selection is performed *separately on each cross-validation fold*. Failure to do so will induce a gene selection bias that yields overly optimistic cross-validation error rates⁴.

5. Results

5.1. Software

The software for the regularized least squares hyperplane classifiers was written in MATLAB. The MATLAB Regularization Toolbox²⁰ was used to calculate the CG-based filter factors for the PLS algorithm.

5.2. Classification performance

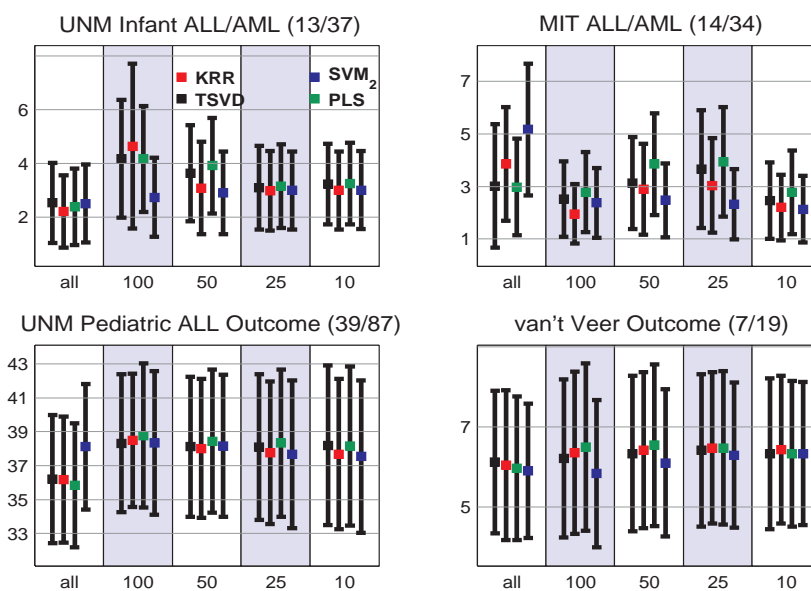
5.2.1. Performance averaged across many partitions

In gene expression studies, a single partition of the training and test set is often used for training and validation. This specific partition is primarily chosen on the basis of case-control considerations in order to mitigate any bias that may arise from the way the patient samples were collected. However, drawing conclusions about classifier performance on the basis of a single training and test set partition can be misleading, especially when the sample size n is small relative to the number of dimensions d . To avoid this dilemma, we measure classifier performance, on average, across many training and test set partitions. To maintain consistency across partitions, the number of positive and negative samples in the training and test set are kept the same. Overall classification performance was measured as an average across 1000 training and test set partitions. The average number of misclassifications was computed as $\bar{M} = (\sum_{p=1}^{1000} M^p)/1000$ in which M^p is computed as in Eq.(1) for the p^{th} training or test set partition.

5.3. Trends in overall classification performance

For each data set, Fig.(2) displays the average number of misclassifications (and corresponding error bars given by the standard deviation) for four different hyperplane classifiers and five distinct feature-set choices (number of genes). Three out of the four classifiers correspond to the standard least squares techniques (TSVD, KRR and PLS) and the fourth classifier corresponds to the two-norm SVM formulation of Eq.(11), hereafter denoted as SVM₂. The average number of misclassifications for each data set is compared to the number of misclassifications that would be obtained by majority class prediction (MCP), where a prediction for a new sample is determined solely by siding with the class in the test set that has the most members (this is not known *a priori*).

Fig. 2. For a given data set, the average number of test set misclassifications (y -axis) was plotted as a function of the number of genes (x -axis). Different colors correspond to different hyperplane classifiers: **black** for SVM_2 , the two-norm SVM of Eq.(11), and **red**, **blue** and **green** for the SVD-based filter factor representations of TSVD, KRR and PLS, respectively. The squares correspond to the average number of misclassifications and the vertical bars indicate the standard deviation. The numbers in parentheses next to the plot title denote the number of misclassifications that would be obtained by majority class prediction (MCP) and the total number of test samples used for that specific data set, respectively.



In Fig.(2), the subplots in rows one and two correspond to the data sets associated with tumor lineage and outcome, respectively. As expected, class prediction tasks related to tumor lineage are ‘easy’ (as evidenced by the low number of misclassification and small standard deviations) since tumor lineage dominates the expression behavior. For outcome, however, the results were only slightly better than what would be obtained by MCP. On average, the choice of regularization scheme did not impact class prediction performance. The simplest of the filter factor strategies, the TSVD scheme, sufficed in most instances.

Somewhat surprisingly, gene selection did not improve performance. In fact, gene selection slightly degraded performance for outcome prediction as the number of genes was decreased. For tumor lineage, only KRR and SVM_2 slightly benefited from gene selection for $d' < 100$. This is not too surprising since KRR and SVM_2 share the same regularization mechanism, *i.e.* the Franklin regularization scheme.

Particularly striking was the poor performance of the least squares classifiers relative to SVM₂ for $d' = 100$ in the **UNM Infant ALL/AML** data set. In this instance, the average number of support vectors was 83 patient samples out of a total of 89 training set samples. Since every patient expression vector is a support vector for the regularized least squares classifiers, “outlier” patient expressions vectors (perhaps the 6 non-support vectors not used by SVM₂) can possibly tilt the weight vector $\hat{\mathbf{w}}$ in such a way that does not generalize well to new data points. Aside from this one instance, the regularized least squares classifiers, compared against SVM₂, were competitive in terms of prediction accuracy, considerably simpler to implement, and faster in terms of execution time. Since TSVD sufficed in most instances, we will now examine its behavior in detail.

5.4. *Spectral coefficients*

The comparable classification performance of TSVD relative to its other, more complicated, filter factor rivals suggests that the type of numerical ill-posedness exhibited by the LS problems derived from the cancer expression data sets in this study tends towards rank-deficiency as opposed to discrete ill-posedness. However, classification performance alone is not the only benchmark measure that can be used to assess whether LS problems, derived from cancer expression data, tend toward rank-deficiency in general. The *spectral coefficients* in Eq.(5) can also be used to indicate the type of numerical ill-posedness. The spectral coefficients consist of the singular values ($\{\sigma_1, \dots, \sigma_n\}$) and the Fourier coefficients ($\{|\mathbf{u}_i^T \mathbf{y}|, \dots, |\mathbf{u}^T \mathbf{y}|\}$). Both of these coefficients decrease in value as i increases and, by examining their rates of decay, they shed insight into the type of numerical ill-posedness of the LS problem. In addition, one can use the decay behavior of these coefficients in estimating the truncation parameter for TSVD. The utility of these coefficients in determining the type of numerical ill-posedness and the TSVD truncation parameter for hyperplane classification of cancer gene expression data is discussed next.

5.4.1. *Gaps in the singular values*

As mentioned previously in Section 3.5, rank-deficiency is characterized by a large gap between singular values σ_k and σ_{k+1} such that $f_i = 1$ for $i \in \{1, \dots, k\}$ and $f_i = 0$ otherwise. In such a case, a general rule of thumb would be that the index of where the gap occurs (*i.e.* k) corresponds to the truncation parameter for TSVD. We now want to see if there is a large gap in the averaged singular value spectrum across all training set partitions such that $\bar{\sigma}_i = (\sum_{p=1}^{1000} (\sigma_i^p)^2) / 1000$, $i = 1, \dots, n$. In Fig.(3) (top row), we have plotted the singular values for varying numbers of genes in each of the four datasets. The averaged rate of decay when using all genes (the solid black line), with the exception of the **UNM Pediatric ALL Outcome** data set, is faster than when using fewer genes. This is to be expected since gene selection should, in principle, remove gene noise by keeping only the most *class-specific* genes. For the **UNM Pediatric ALL Outcome** data set the opposite

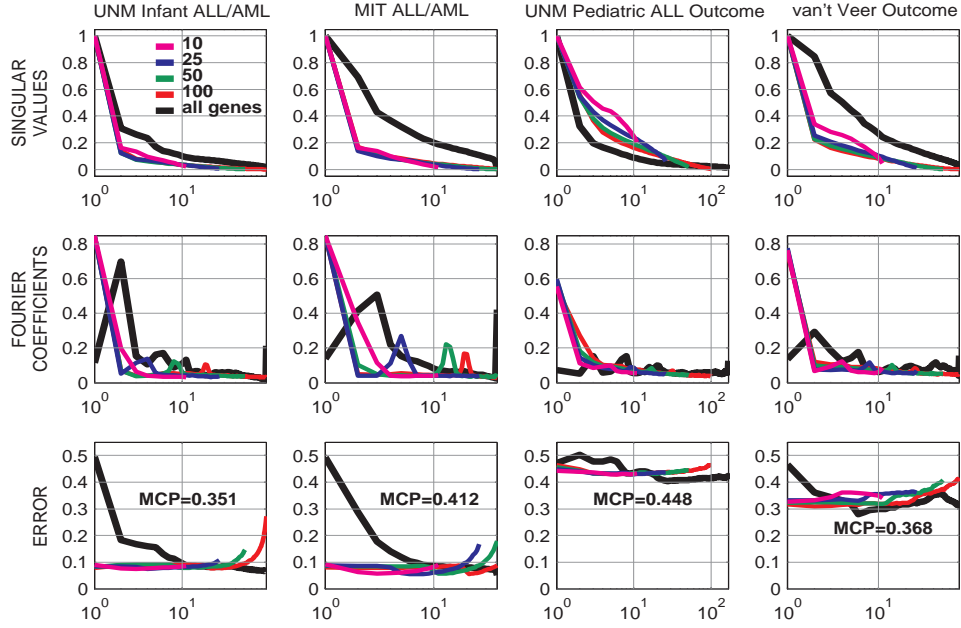
is true: the rate of decay decreases as d' decreases. What could cause this rank inflation as d' decreases in this instance? One possible answer to this question lies in the heterogeneity of this data set. The **UNM Pediatric ALL Outcome** data set can be grouped according to the two major lymphocyte subtypes: B-cells (34 samples) and T-cells (220 samples). They may also be characterized by molecular subtype or chromosomal abnormality (30 t(12;21), 30 t(1;19), 14 t(9;22), 20 t(4;11) and 29 hyperdiploid samples, with 131 'other' molecular subtype samples). Since tumor lineage and chromosomal abnormalities determine the fate of cancer cells, these class distinctions dominate the observed expression behavior in terms of signal recovery. Classifying expression on the basis of these class distinctions is expected to be relatively easy since the gene expression profiles corresponding to different cell or chromosomal subtypes have relatively large signal-to-noise ratios. Indeed, this is borne out in tests^{23,33}. Hence, if one is interested in outcome signal recovery, then one has to contend with the relative weakness of the outcome signal compared to the dominant biological signals of tumor sublineages and molecular subtypes. Furthermore, the gene selection process for outcome may be confounded since the signal-to-noise ratio is low: in essence, one is attempting to find outcome-specific genes by training on noise. Unfortunately, we believe that this hypothesis cannot be adequately addressed using real expression data. Thus, in order to assess whether gene selection techniques actually find the class-specific genes of interest when there are many competing sources of biological variability, a simulation approach will most likely be necessary.

5.4.2. Fourier coefficients

For the four gene expression data sets examined, the decay of the Fourier coefficients proved more illuminating than the singular value decay in terms of determining the type of ill-conditioning. In the presence of noise, the Fourier coefficients $|\mathbf{u}_i^T \mathbf{y}|$ will level off at a base-line level of background noise determined by the errors in the coefficient matrix \mathbf{K} for $1 \leq i_0 < i \leq n$ ¹⁹. As a result, the SVD expansion terms for $i > i_0$ should, in principle, be filtered out since these terms are contaminated by noise and will dominate the OLS solution. Under this criterion, i_0 can be used as a proxy for the TSVD truncation parameter, *i.e.* we set $k \approx i_0$.

The second row of Fig.(3) displays the averaged Fourier coefficients, $\bar{c}_i = (\sum_{p=1}^{1000} |(\mathbf{v}_i^p)^T \mathbf{y}^p|)/1000$, $i = 1, \dots, n$. Note that as the number of genes decreases from $d' = d$ to $d' = \{100, 50, 25, 10\}$ across all four data sets, there is a qualitative change in the decay of \bar{c}_i . When $d' = d$, the decay of \bar{c}_i (given by the solid black line) slowly oscillates toward zero and $i_0 \approx r = \min\{n-1, d'\}$ ($r = n-1$ or nearly full rank when $n < d$ and $r = d$ when $n > d$). This indicates that all terms in the SVD expansion should be kept and the OLS solution would suffice in effectively classifying the expression data. This was experimentally borne out by examining the average number of misclassifications as a function of the truncation parameter,

Fig. 3. For a given data set, the y -axes denote averaged singular values (first row), averaged Fourier coefficients (second row) and averaged number of misclassifications for the TSVD method (third row). The x -axes denote the summation index i or the truncation parameter k in the case of the averaged number of misclassifications. Different colors correspond to the different numbers of genes used in the analysis (see legend).



denoted by $\bar{M}_k = (\sum_{p=1}^{1000} M_k^p) / 1000$, where

$$M_k^p = \sum_{j=1}^N I[t_j^p((\hat{z}_j^p)^T \hat{\mathbf{w}}^{(k,p)})] \left(\hat{\mathbf{w}}^{(k,p)} = \sum_{i=1}^k \frac{(\mathbf{v}_i^p)^T \mathbf{y}^p}{(\sigma_i^p)^2} f_i^p \mathbf{u}_i^p \right) \quad (14)$$

is the number of misclassification per truncation parameter k and partition p . In the third row of Fig.(3), \bar{M}^k is plotted against k . When $k \approx r$ and $d' = d$, the minimum value or a near minimum value for \bar{M}^k was obtained for tumor lineage and outcome, respectively.

When using fewer genes ($d' < d$), the decay of \bar{c}_i (the colored lines) descends quickly to 0 such that $i_0 \approx 1$ (the exception was the **UNM Pediatric ALL Outcome** data set). In this case, $i_0 \approx 1$ implies that a low-rank approximation for \mathbf{K} suffices for effective classification. Again, this was experimentally borne out since $k \approx 1$ was the truncation parameter that minimized \bar{M}_k (in good agreement with the effective resolution limit of $i_0 \approx 1$). Notice that for the **UNM Pediatric ALL Outcome** data set, the Fourier coefficient decay was not as rapid as with

the other data sets (*i.e.* $i_0 \gg 1$). Again, there was good experimental agreement between the value of i_0 and the truncation parameter ($k \gg 1$) that minimized \bar{M}_k in the third row of Fig.(3). While i_0 does appear to be a reasonable proxy for a near-optimal TSVD truncation parameter, caution is still advised in the case of outcome prediction since the best misclassification results were, on average, barely below MCP.

6. Conclusion and Future Work

In this study, we have shown that many popular least squares techniques used for linear discrimination can easily be united under the framework of an SVD-based filter factor representation. Using the philosophy of Occam’s razor as a guide, and based upon the four data sets examined, the TSVD regularization scheme emerged as the preferred hyperplane regularization strategy since its performance was comparable, on average, to SVM₂ and to the other more complicated filter factor strategies. The classification performance of TSVD, coupled with the decay behavior of the Fourier coefficients in Fig.(3), lends credence to the observation that linear inverse problems associated with the hyperplane classification of gene expression data tend toward rank-deficiency as opposed to discrete ill-posedness, especially when using fewer genes. The spectral coefficients, in particular the Fourier coefficients, act as useful numerical diagnostics, indicating when signal recovery for outcome or tumor subclass is possible.

Gene selection did not necessarily lower the number of misclassifications. Indeed, for outcome, the best performance was often achieved using all d genes. One possible explanation is that the genes responsible for distinguishing differences in outcome are dominated by a significant number of differentially expressed genes responsible for the major sources of *upstream* biological variation, *e.g.* tumor subclass distinctions or molecular subtype in the case of leukemia. If this is the case, signal recovery for outcome is likely to be severely hampered because the major sources of variation (biological and experimental) can inflate the singular value spectrum to such an extent that the only signals that remain above the noise background are those which dominate the expression behavior. The testing of this hypothesis will require extensive gene array simulations and the modeling of cancer gene expression as a superposition of tumor subclass, outcome and experimental set effect signals, with class-specific sets of genes responsible for distinguishing class subtypes within each signal. This is a subject for future study. Alternatively, one can restrict the patient sample size to create data subsets that are less heterogeneous in terms of dominant sources of variation, *i.e.* gene selection within samples restricted to B-cell or T-cell acute lymphoblastic leukemias only. However, one then pays the price of working with data sets that are of extremely small size. In general, gene selection, by preserving the most class-specific genes, allows for very aggressive regularization by making the kernel matrix more rank-deficient—as indicated by the rapid decay of the Fourier coefficients from $d' = \{\text{all genes}\}$ to $d' \leq 100$ genes. This results in

the ability to construct low-rank approximations of the kernel matrix \mathbf{K} .

The main reason for the success of SVD as an analysis tool is that it provides a new coordinate system in which the coefficient matrix \mathbf{K} becomes diagonal (*i.e.* $\mathbf{\Sigma} = \text{diag}(\sigma_1, \dots, \sigma_n)$). As a consequence, SVD is *rank-revealing*: the largest singular values and vectors capture the relevant solution information by eliminating or downweighting noise terms (using filter factors) in the SVD expansion associated with the smallest singular values. However, there are alternatives to the SVD, *i.e.* there exist other rank-revealing matrix factorization techniques such as rank-revealing QR or UTV factorizations¹⁹ that can also reliably solve rank-deficient LS problems. Since TSVD works well with regularized LS techniques in classifying gene expression data, it is likely that these alternative matrix factorizations will work just as well. Moreover, and unlike SVD, these alternative matrix factorizations permit for the efficient updating of rows and columns when they are appended or deleted from \mathbf{K} ¹⁹, a common scenario in gene expression studies since patients and genes are routinely added or deleted from analysis as new clinical and experimental information becomes available. Investigations of such alternative factorization approaches in hyperplane classifiers is currently in progress.

Acknowledgements

This work was supported in part by grants from the D.H.H.S. National Institute of Health NCI CA88361 and NCI CA32102, the W.M. Keck Foundation, and funds from the Dedicated Health Research Fund of the State of New Mexico. This work was also supported in part by NSF Grant DMS-0306285. Any conclusions or recommendations expressed in this paper are those of the author and do not necessarily reflect the views of the NSF. Erik Andries would like to acknowledge the UNM Center for High Performance Computing (CHPC) for graduate fellowship support. The authors also thank the CHPC for providing the computational resources used in this work.

References

1. *Statistical Algorithms Reference Guide*, Affymetrix Corporation, Santa Clara, CA, www.affymetrix.com/support/technical/technotes/statistical_reference_guide.pdf.
2. Agarwal D, Shrinkage estimator generalizations of proximal support vector machines, In *Proceedings of the Eighth ACM SIGKDD International Conference on Knowledge Discovery and Data Mining*, Eds. Hand D, *et al.*, Edmonton, Canada, 173-182, 2002.
3. Alter O, Brown PO, Botstein D, Singular value decomposition for genome-wide expression data processing and modeling, *Proc. Natl. Acad. Sci. USA*, **97**(18):10101-10106, 2000.
4. Ambrose C, McLachlan G, Selection bias in gene extraction on the basis of microarray gene-expression data, *Proc. Natl. Acad. Sci. USA*, **99**(10):6562-6566, 2002.
5. Aster R, Borchers B, Thurber C, *Parameter Estimation and Inverse Problems*. Academic Press, 2004.
6. Bair E, Hastie T, Paul D, Tibshirani R, Prediction by supervised principal components, *Technical report, Stanford University, September 2004*.

7. Bertsekas D(1999). *Nonlinear Programming*. Athena Scientific, Singapore.
8. Carroll WL, Bhojwani D, Min D-J, Raetz E, Relling M, Davies S, Downing JR, Willman CL, Reed JC, Pediatric acute lymphoblastic leukemia, *Hematology*, 102-131, 2003.
9. Cristianini N, Shawe-Taylor J, *An Introduction to Support Vector Machines*, Cambridge University Press, Cambridge, UK, 2000.
10. Demmel JW, *Applied Numerical Linear Algebra*, SIAM Press, Philadelphia, 1997.
11. Dudoit S, Fridlyand J, Speed T, Comparison of discrimination methods for the classification of tumors using gene expression data, *JASA*, **97**(457):77-87, 2002.
12. Franklin JN, Minimum principles for ill-posed problems, *SIAM J. Math. Anal.*, **9**(4):638-650, 1979.
13. Fung G, Mangasarian O, Proximal support vector machines, *Data Mining Institute Technical Report 01-02*, 2001.
14. Ghosh D, Singular value decomposition regression modelling for classification of tumors from microarray experiments, In *Proceedings of the 2002 Pacific Symposium on Biocomputing*, Eds. Altman, RB *et al.*, Honolulu, USA:18-29, 2002.
15. Golub T *et al.*, Molecular classification of cancer: class discovery and class prediction by gene expression monitoring, *Science*, **285**:531-537, 1999.
16. Golub G, Hansen PC O'Leary D, Tikhonov regularization and total least squares. *SIAM J. Matrix Anal. Appl.*, **21**(1):185-1940, 2002.
17. Guo H, Renaut RA, Efficient algorithms for the solution of regularized total least squares, *SIAM J. Matrix Analysis*, **26**(2):457-476, 2005.
18. Guyon I, Weston J, Barnhill S, Vapnik V, Gene selection for cancer classification using support vector machines, *Machine Learning*, **46**:389-422, 2002.
19. Hansen PC, *Rank-deficient and discrete ill-posed problems*, SIAM Press, Philadelphia, 1998.
20. Hansen PC, Regularization tools: a MATLAB package for analysis and solution of discrete ill-posed problems. *Numerical Algorithms*, **6**:1-35, 1994.
21. Hastie T, Tibsharani R, Friedman J, *The Elements of Statistical Learning*, Springer-Verlag, New York, 2001.
22. Helland I, On the structure of Partial Least Squares, *Commun. Statist. Simulation Comput.*, **17**:581-607, 1988.
23. Kang H, Atlas SR, Li B-L, Bedrick EJ, Willman C, Statistical methods for evaluating the performance of class predictors in gene expression analysis, University of New Mexico Center for High Performance Computing Technical Report HPC@UNM 2004-003, submitted, 2005.
24. Khan J *et al.*, Classification and diagnostic prediction of cancers using gene expression profiling and artificial neural networks, *Nature Medicine*, **7**(6):674-679, 2001.
25. Lingjærde O, Christopherson N, Shrinkage structure of partial least squares. *Scandinavian Journal of Statistics*, **27**:459-473, 2000.
26. Mangasarian OL, Musicant DR, Lagrangian Support Vector Machines, *Journal of Machine Learning Research*, 1:161-177.
27. Nguyen D, Rocke D, Tumor classification by partial least squares using microarray gene expression data, *Bioinformatics*, **18**(1):39-50, 2002.
28. Trefethen L, Bau III D, *Numerical Linear Algebra*, SIAM Press, Philadelphia, 1997.
29. UNM ALL cohort, Data available at the **National Cancer Institute Gene Expression Data Portal**, <http://gedp.nci.nih.gov/dc>. Experiment Id: 754.
30. UNM Infant cohort, Data available at the **National Cancer Institute Gene Expression Data Portal**, <http://gedp.nci.nih.gov/dc>. Experiment Id: 755.
31. Varah J, Pitfalls in the numerical solution of linear ill-posed problems, *SIAM J. Sci. Stat. Comput.*, **4**(2):164-176, 1983.

32. van't Veer L *et al.*, Gene expression profiling predicts clinical outcome of breast cancer, *Nature*, **415**:530-536, 2002.
33. Willman CL, Discovery of novel molecular classification schemes and genes predictive of outcome in leukemia, *The Hematology Journal*, **5**:S138-S143, 2004.
34. Yeoh E *et al.*, Classification, subtype discovery, and prediction of outcome in pediatric acute lymphoblastic leukemia by gene expression profiling, *Cancer Cell*, **1**(2):133-143, 2002.
35. Jaffe ES, Harris NL, Stein H, Vardiman JW, eds. World Health Organization Classification of Tumors of Haematopoietic and Lymphoid Tissues, IARC Press, Lyon, France, 2001.